

STEADY STATE ANALYSIS OF GRID CONNECTED WIND ENERGY CONVERSION SYSTEMS

S.G.BHARATHI DASAN

Senior lecturer-Department of Electrical and Electronics Engineering,
Sri Venkateswara College of Engineering, Sriperumbudur, India
Email: vaigaibharathi@rediffmail.com

Dr.R.P.KUMUDINI DEVI

Assistant Professor-Department of Electrical and Electronics Engineering,
College of Engineering, Guindy, Anna University, Chennai, India

Abstract: To fulfill the increasing power requirement, in an eco-friendly manner, a large number of wind farms are already in operation and more are planned or under construction. Variable speed systems with power electronic interface take over the disadvantages of fixed speed wind generators. This paper presents the performance analysis comparison of fixed speed (SCIG-Squirrel cage induction generator) and variable speed (DFIG-Doubly-fed induction generator) wind generators interconnected to the grid when they treated as PQ bus. This study also makes use of the ability of variable speed systems to extract maximum power from the available wind power. On the other hand, power system dynamic study is very much essential to study the influence of wind turbines on electrical power systems. This transient study requires initialization of state variables. The proposed approach is a simple method which requires minimum effort to initialize the state variables of DFIG for transient stability analysis.

Keywords: SCIG, DFIG, MPPT, Fixed-Speed, Variable-speed.

NOMENCLATURE

P_m - power extracted from the wind turbine,
 ρ - Density of air in kg/m^3
 A - Rotor swept area in m^2
 C_p - power coefficient,
 u_w - wind speed in m/s
 λ - tip speed ratio
 R - Radius of wind turbine
 ω - Rotor speed
 θ - Pitch angle
 λ_{opt} - Optimum value of tip speed ratio
 ω_{opt} - Optimum value of rotor speed
 s - Per unit value of slip
 ω_s - Synchronous speed

P_e – Air gap power of induction generator
 R_s – Stator resistance
 R_r – Rotor resistance
 X_s – Stator leakage reactance
 X_r – Rotor leakage reactance
 X_m – magnetizing reactance
 T_m - Mechanical torque of wind turbine
 T_e - Electromagnetic torque of generator
 P_r - Active power injected on to the rotor
 I_r - Rotor current
 I_s - Stator current
 $i_{dr} \& i_{qr}$ - Direct and Quadrature components of rotor currents
 V_r - Injected rotor voltage
 $V_{dr} \& V_{qr}$ - Direct and Quadrature components of rotor voltages
 V_s - Stator terminal voltage
 $V_{ds} \& V_{qs}$ - Direct and Quadrature components of stator terminal voltages

1. INTRODUCTION

While attempting to meet increase in demand, as a result of increasing environmental concern, more and more electricity is generated from renewable sources. One of the most popular ways of generating electricity from renewable sources is to use wind turbines. The need of extracting more power from the available wind power forces the application of different technologies in conversion systems.

There are basically three types of generators that are commonly used with commercial wind turbines. They are (1) fixed-speed system with squirrel-cage

induction generator, (2) variable-speed system with Doubly-Fed Induction Generator (DFIG) (3) variable-speed system with a direct-drive synchronous generator. DFIG based variable speed wind energy conversion systems are currently the most admired one, due to its high energy efficiency and due to the fact that a inverter with a rating of only 20%–30% of the rated Wind turbine power is needed [1].

In [2], two methods for the simulation of wind farms with asynchronous generators in the load flow analysis. Both methods are based on the steady state model of the induction machine. The first involves improving the conventional PQ bus and the second involves modelling of the generators by means of a RX bus, in which the induction generator is simulated as impedance. Divya [3] developed steady state models for various types of WECS for load flow analysis. She also demonstrated the application of these models for both deterministic and probabilistic load flow analysis.

In [4], variable-speed system with DFIG is analysed when it supplies an isolated load. Two back-to-back PWM voltage-fed inverters connected between rotor and the grid allows both sub-synchronous and super-synchronous operation. Holds [5], presented a direct solution method for initialising doubly-fed induction generator in power system dynamic models. In [6], the performance of fixed-speed and variable-speed asynchronous generator wind turbines during power system disturbances is dealt. Both fixed-speed (squirrel-cage) and doubly-fed (wound rotor) machine constructions are represented by a set of equations, differing only by the representation of rotor voltage. Slootweg [7] suggested a method to initialise the state variables of different WECS concepts for transient stability analysis.

This paper presents the performance analysis comparison of fixed speed (SCIG) and variable speed (DFIG) wind generators and their impact on the grid after grid integration. A new simple method is proposed for initialising the state variables of variable speed (DFIG) wind generators in transient stability simulations.

The section 2 describes the wind turbine model and MPPT algorithm, section 3 explains about the steady state analysis of fixed speed and variable speed wind generators, section 4 discusses the

different modes of DFIG operation, section 5 provides the simulation results, section 6 describes initialization of state variables of DFIG using obtained results and section 7 concludes the paper.

2. WIND TURBINE MODEL

The general structure of wind generator as shown in the Fig.1.

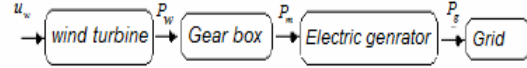


Fig. 1 General structure of wind generator

The power extracted from the wind turbine is

$$P_m = \frac{1}{2} \rho A u_w^3 C_p \quad (1)$$

where, P_m - power extracted from the wind turbine,
 ρ - Density of air in kg/m^3
 A -Rotor swept area in m^2
 C_p - power coefficient
 u_w - wind speed in m/s

The tip-speed ratio is given by,

$$\lambda = \frac{\omega R}{u_w} \quad (2)$$

where, u_w is the wind speed, R is the radius of the turbine rotor and ω is the rotor speed. A general functional representation of C_p is given in [7].

$$C_p(\lambda, \theta) = C_1 \left(\frac{C_2 - C_3 \theta - C_4 \theta^x - C_5}{\lambda} \right) e^{\frac{-C_6}{\lambda}} \quad (3)$$

where,

$$\frac{1}{\lambda} = \frac{1}{\lambda + 0.008 \theta} - \frac{0.035}{1 - \theta^3} \quad (4)$$

$C_1, C_2, C_3, C_4, C_5, C_6$ and x are constants. The C_p versus λ curve is provided by the manufacturer.

2.1 MPPT algorithm for DFIG

Maximum power point tracking (MPPT) is the main attraction of variable speed systems. To extract the maximum power from available wind using DFIG, an MPPT algorithm is presented. The maximum power occurs at an optimum value of tip-speed ratio λ_{opt} . The schematic diagram of DFIG for obtaining maximum power extraction at different wind speeds is shown in Fig.2.

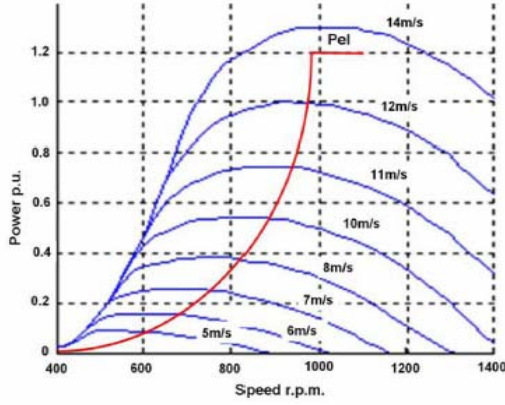


Fig.2. Maximum power extraction of a wind generator

The power coefficient shown in equation (3) is a function of tip-speed ratio and pitch angle and the power extracted from wind shown in equation (1) is a function of Power coefficient. Therefore to find the value of λ_{opt} , we differentiate the equation (1) with respect to λ_{opt} and equate to zero to get

$$\frac{dP_m}{d\lambda_{opt}} = \frac{1}{2} \rho A u_w^3 \frac{dC_p(\lambda, \theta)}{d\lambda_{opt}} = 0 \quad (5)$$

By solving the equation (5), we will get the optimum value of tip-speed ratio is

$$\lambda_{opt} = \frac{1}{\left(\frac{1}{c_6}\right) + \left(\frac{c_5}{c_2}\right) + \left(\frac{c_3 * \theta}{c_2}\right) + \left(\frac{0.035}{1 - \theta^3}\right)} - (0.008 * \theta) \quad (6)$$

From the optimum value of tip-speed ratio we will get optimum value of rotor speed is

$$\omega_{ropt} = \frac{\lambda_{opt} * u_w}{R} \quad (7)$$

From the optimum value of rotor speed we obtain the optimum value of slip is

$$s = \frac{\omega_s - \omega_{ropt}}{\omega_s} \quad (8)$$

3. STEADY STATE MODEL OF SCIG & DFIG

3.1 Steady state model of fixed speed (SCIG) wind generator.

The steady state equivalent circuit model of the SCIG is shown in Fig.3. The model considered here is a squirrel cage induction generator and is directly connected to the grid. In the operating range the

rotor speed varies within a very small range (around 1-5% of the nominal value) and hence, these are known as fixed speed generators.

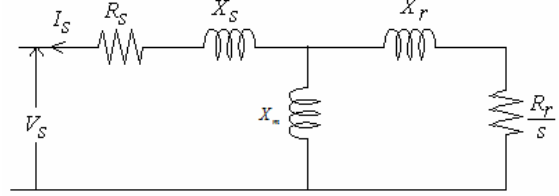


Fig. 3 Steady state equivalent circuit of fixed speed wind generator

From the equivalent circuit the expression for the air gap power is obtained as

$$P_e = \left| I_r \right|^2 \frac{R_r}{s} \quad (9)$$

In fixed speed (SCIG) wind generators slip 's' is considered as a state variable and power flow is conducted until $P_m = P_e$.

3.2 Steady state model of variable speed (DFIG) wind generator

The approximate equivalent circuit model of the DFIG is shown in Fig.4

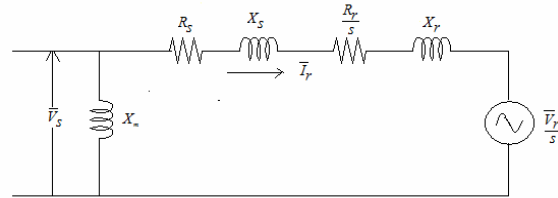


Fig. 4 Approximate steady state equivalent model with injected rotor voltage.

However, in this paper a direct solution method has been derived using torque and reactive power balance equations (16) and (18) to reduce computation time in large power system studies.

3.2.1 Steady state electric torque control

A starting point for the direct solution is the steady state torque balance equation with the mechanical loss torque neglected is [5].

$$\overline{T_m} = \overline{T_e} \quad (10)$$

The electromagnetic torque of DFIG is derived as

$$\overline{T_e} = \overline{i_r} \frac{-2}{s} \frac{R_r}{s} + \frac{\overline{P_r}}{s} \quad (11)$$

where the active power injected onto the rotor side is calculated from

$$\overline{P_r} = \Re \left(\overline{V_r}^* \overline{i_r} \right) \quad (12)$$

The rotor current for the DFIG from equivalent circuit is

$$\overline{i_r} = \frac{\overline{V_s} - \overline{V_r}}{s \left(R_s + \frac{R_r}{s} \right) + j(X_s + X_r)} = \overline{i_{dr}} + j\overline{i_{qr}} \quad (13)$$

The electromagnetic torque components are derived as follows

$$\overline{i_r} \frac{-2}{s} \frac{R_r}{s} = (H_1^2 + H_2^2) K_3 \quad (14)$$

$$\frac{\overline{P_r}}{s} = -(H_1^2 + H_2^2) K_1 + K_4 H_1 + K_5 H_2 \quad (15)$$

By substituting (14) and (15) into (11), the torque balance equation (10) is expressed as

$$(K_3 - K_1)(H_1^2 + H_2^2) + K_4 H_1 + K_5 H_2 - \overline{T_m} = 0 \quad (16)$$

3.2.2 Steady state power factor control

The solution of the steady state power factor control is derived through the formulation of a reactive power balance equation. [5]

$$\overline{Q_s} - \frac{\overline{V_s}^2}{X_m} = \left| \overline{P_s} \tan \theta \right| - \frac{\overline{V_s}^2}{X_m} = \Im \left(\overline{V_s} \overline{i_r}^* \right) = \overline{V_{qs}} \overline{i_{dr}} - \overline{V_{ds}} \overline{i_{qr}} \quad (17)$$

By algebraic substitution of variables the reactive power balance equation is expressed as

$$K_8 H_1 + K_9 H_2 + \frac{\overline{V_s}^2}{X_m} = 0 \quad (18)$$

3.2.3 Direct solution for injected rotor voltage components

From the reactive power balance equation (18) we find that H_2 has an algebraic relationship with H_1 [5]. Substituting the relationship for H_2 into the torque balance equation (16) results in only one unknown H_1 , which is solved using the quadratic equation given below

$$H_1 = \frac{-b \pm \sqrt{b^2 - 4ac}}{2a} \quad (19)$$

where the quadratic equation variables are defined by

$$\begin{aligned} a &= (K_3 - K_1)(1 + K_{10}^2) \\ b &= 2(K_3 - K_1)K_{10}K_{11} + K_4 + K_5K_{10} \\ c &= (K_3 - K_1)K_{11}^2 + K_5K_{11} - \overline{T_m} \end{aligned} \quad (20)$$

The negative solution of H_1 for super synchronous generating mode and the positive solution of H_1 for sub synchronous generating mode gives a variation of $\overline{V_{dr}}$ and $\overline{V_{qr}}$ are within the converter voltage limits. By substitution of the value of H_1 into the algebraic relationship for H_2 from the reactive power balance equation (18), a solution for H_2 is found. Using these two variables, the injected rotor voltage components are derived as

$$\begin{aligned} \overline{V_{dr}} &= s(\overline{V_{ds}} - H_1) \\ \overline{V_{qr}} &= s(\overline{V_{qs}} - H_2) \end{aligned} \quad (21)$$

4. DFIG MODES OF OPERATION

The Doubly fed induction generator operates in modes of operation [9].

1. Sub Synchronous generating mode
2. Super Synchronous generating mode

In sub synchronous generating mode the stator fed power to the grid whereas rotor draws power from grid shown in Fig.6.

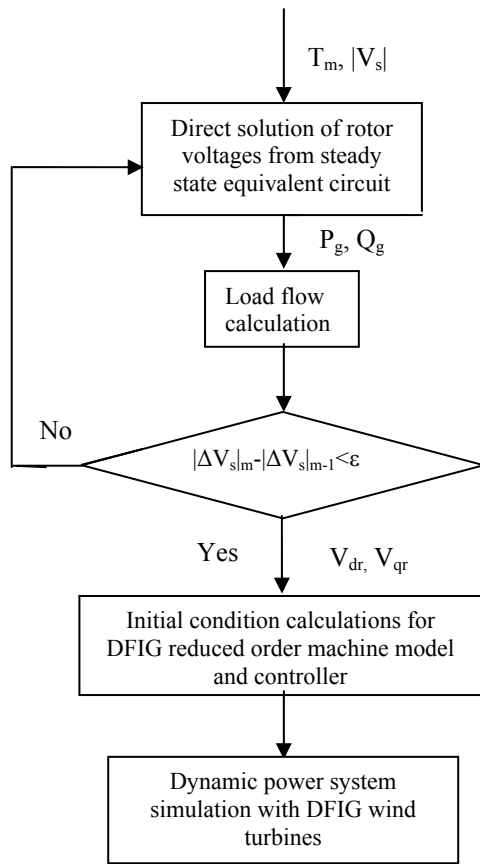


Fig.5 Flow chart of DFIG as a PQ bus for initializing injected rotor voltages for dynamic simulations.

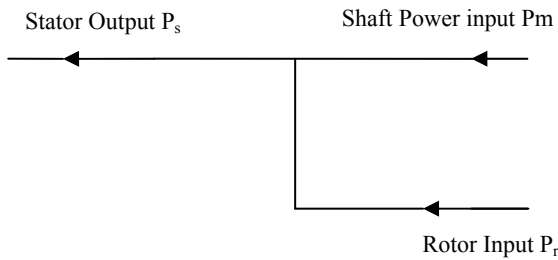


Fig.6 Power flow diagram of Sub Synchronous Generating mode

In Super Synchronous generating mode the stator as well as the rotor both fed power to the grid shown in Fig.7.

5. SIMULATION RESULTS

The single line diagram of 9-bus radial system [8] is shown in the Fig. 8.

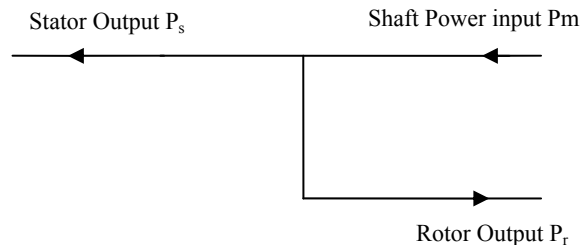


Fig. 7 Power flow diagram of Super Synchronous generate mode.

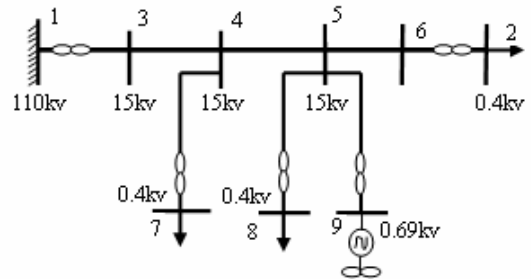


Fig.8 .Single line diagram of 9-bus radial system

5.1 Power flow results of Variable-Speed (DFIG) wind generator

The power flow results of DFIG at wind speed 5m/s is shown in the following Table.1.

From wind speeds 11m/s to 25m/s the blade pitch angle is adjusted to keep the power output to the grid is equal to rated power. The initial values of injected rotor voltages are calculated by using the equation (21), which are within the converter voltage limits.

Table.1 Power flow results of DFIG at wind speed 5 m/s

	Voltage (P.u)	Angle (deg)	P _g (kW)	Q _g (kVAR)
1	1.000	0	404.25	439
2	0.934	-1.273	0	0
3	0.998	-0.097	0	0
4	0.975	-0.301	0	0
5	0.960	-0.400	0	0
6	0.951	-0.508	0	0
7	0.958	-1.030	0	0
8	0.943	-1.152	0	0
9	0.960	-0.270	60.25	0

The power flow results of DFIG with two modes are shown in the following Table 2.

Table. 2. Power flow results of DFIG at different wind speeds

Wind speed (m/s)	Stator Power P_s (kw)	Rotor Power P_r (kw)	Total power (kw)	Slip s (p.u)
5	80	-19.75	60.25	0.2667
6	140	-37.5	102.5	0.2667
7	220	-40	180	0.1882
8	330	-22.5	307.5	0.0723
9	470	22.25	492.25	-0.0437
10	647.5	107.5	755	-0.1597
11-25	-	-	855	-0.2667

5.2 Comparison of Fixed-Speed (SCIG) and Variable-Speed (DFIG) wind generators.

Simulations are carried out for wind speeds ranging from 5 m/s (cut-in speed) to 25 m/s (cut-out speed) in steps of 2 m/s with one wind turbine (SCIG or DFIG) connected at a time at bus 9. The variation of real power generated for both SCIG and DFIG at different wind speeds are presented in Table 3.

From Table 3 it can be noted that with SCIG the power output increases from with the wind speed increasing from cut-in(5m/s) to rated wind speed(17m/s) and decreases thereafter up to cut-off. Also maximum power is obtained at rated wind speed (17m/s). In the case of DFIG the power output is less at low wind speeds (5 m/s -8m/s) as compared to SCIG. Since the DFIG operates in sub-synchronous generating mode. From wind speeds 9 m/s to 25 m/s DFIG operates in super- synchronous generating mode, therefore the power output to grid is more than the SCIG.

The variation of real power generated for both SCIG and DFIG at different wind speeds is shown in the Fig. 9.

Table 3 Variation of Real power generated with respect to wind speeds for both SCIG & DFIG

Wind speed (m/s)	Real Power Generated P_g (SCIG)	Real Power Generated P_g (DFIG)
5	86	60.25
7	219	180
9	381.25	492.83
11	536.75	855
13	660.50	855
15	741.25	855
17	778.50	855
19	777.75	855
21	747.50	855
23	697.25	855
25	635.25	855

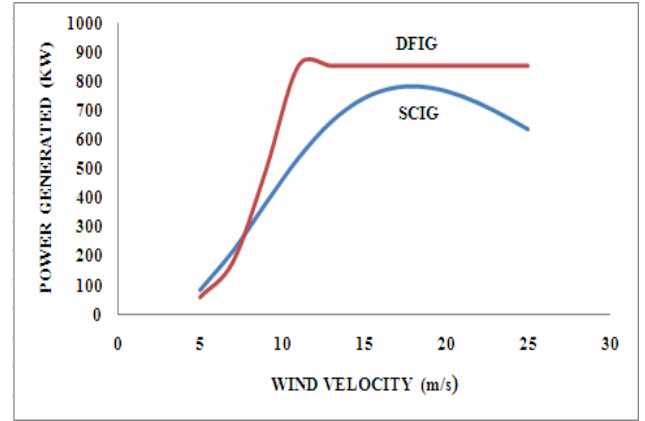


Fig. 9 Variation of realpower generated with respect to wind speed.

6. INITIALIZATION OF STATE VARIABLES

6.1. Need for initialization of state variables

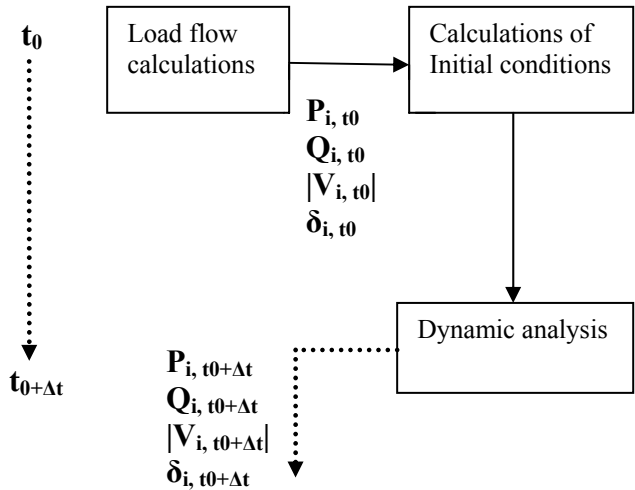


Fig.10. Dynamic Simulation activity sequence

Normally, calculations of Initial conditions of dynamic equipment models are made based on load flow results. If this is not done correctly, state variables and other quantities do not stay at the value at which they are initialized but start changing at the start of dynamic simulation. In this situation, it may take much time to reach new equilibrium and numerical stability can occur before equilibrium is reached, it can be different from original load flow case that was initially planned to be investigated. These are undesirable [7]

Here, a simple method is proposed to initialize the state variables of DFIG for transient stability analysis. The steady state exact equivalent circuit of variable speed (DFIG) is shown in Fig.11.

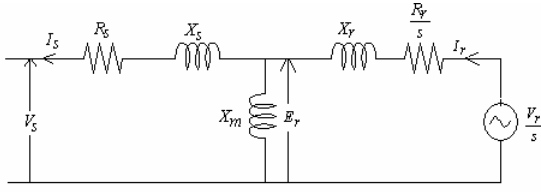


Fig .11 Steady state exact equivalent circuit of DFIG

Let us consider the DFIG power output to the grid is

$$P_s + P_r = \eta P_{\max} \quad (22)$$

where

P_s = Stator power in pu

P_r = Rotor power in pu

P_{\max} = Maximum power from MPPT

η = Efficiency.

The efficiency of the DFIG is assumed as 85%, therefore the power output to the grid is a known quantity and also assumed the reactive power of DFIG is equal to zero. With known quantities of P and Q the DFIG is treated as PQ bus. The normal power flow results of DFIG at wind speed 5m/s is shown in the following Table 4.

Now with the known voltage magnitude and angle at 9th bus we calculated the voltage E_r by using the following equation

$$E_r \angle \alpha = \overline{V_s} \angle \theta - \overline{I_s} (R_s + jX_s) \quad (23)$$

Now the injected rotor voltage is calculated by using the following equation

$$\frac{\overline{V_r}}{s} \angle \beta = E_r \angle \alpha + \overline{I_r} \left(\frac{R_r}{s} + jX_r \right) \quad (24)$$

Where the slip is a known quantity calculated from MPPT described in section 2.1.

The values of V_{dr} and V_{qr} by using both direct solution method [5], and proposed method are compared and tabulated in the following Table 5.

Table4. Network profile for PCC as a PQ bus.

Bus no	Voltage (P.u)	Angle (deg)	P_g (kw)	Q_g (kvar)
1	1.000	0	396.75	438.75
2	0.934	-1.242	0	0
3	0.998	-0.095	0	0
4	0.975	-0.285	0	0
5	0.960	-0.370	0	0
6	0.952	-0.477	0	0
7	0.958	-1.014	0	0
8	0.943	-1.121	0	0
9	0.961	-0.223	67.5	0

Table 5. Comparison between the initialisation of rotor voltages

Method	Voltage (p.u)	Angle (deg)	V_{dr} (p.u)	V_{qr} (p.u)
Direct solution method	0.961	-0.223	0.264	-0.005
Proposed method	0.960	-0.270	0.268	-0.006

7. CONCLUSION

The steady state model of fixed-speed (SCIG) and variable-speed (DFIG) wind turbine has been described. An MPPT algorithm was described for maximum power extraction from the DFIG. A direct solution method has been derived from the steady state model of DFIG for obtaining the injected rotor voltages (V_{dr} , V_{qr}) to initialise the dynamic DFIG wind turbine model [5]. The SCIG & DFIG was represented as a PQ bus and simulations were carried out from wind speeds 5m/s to 25m/s on a 9-bus radial system [8].

The two modes of operation of DFIG i.e. sub synchronous generating mode and super synchronous generating mode are presented. From the steady state analysis of both fixed-speed (SCIG) and variable speed (DFIG), we concluded that the DFIG generates more power compare to SCIG, since in DFIG the rotor also fed power to the grid. A simple method was also proposed for initialising the DFIG rotor voltages in transient stability simulations and compared with the direct solution method described in [5].

ACKNOWLEDGEMENT

Authors acknowledge Mr.M.SivakoteswaRarao, PG student of College of Engineering, Guindy for the help rendered in developing MATLAB code. Authors thank management and faculty of SVCE and CEG-Guindy for their support and encouragement.

APPENDIX-A

A 1 Line data

Parameter	Value	Unit
Resistance	0.24	Ω/km
Reactance	0.36	Ω/km
Susceptance	2.8	$2.8\mu\text{s}/\text{km}$
Length	20	Km

A 2 Load data

All loads
0.150+j0.147 MVA

A 3 Wind generator data (DFIG)

Parameter	Value
Gear box ratio	65.27
Blade radius	28.5m

A 3.1 Power coefficients

$C_1=0.5$	$C_4=0$
$C_2=116$	$C_5=5$
$C_3=0.4$	$C_6=21$

A 3.2 DFIG data

Parameter	Value
Stator resistance	0.0027 Ω
Rotor resistance	0.0022 Ω
Stator leakage reactance	0.025 Ω
Rotor leakage reactance	0.046 Ω
Magnetizing reactance	1.38 Ω

A 4 Wind generator data (SCIG)

Parameter	Value
Gear box ratio	67.5
Blade radius	26.1m

A 4.1 Power coefficients

$C_1=0.5$	$C_4=0$
$C_2=67.56$	$C_5=1.517$
$C_3=0$	$C_6=16.286$

A 4.2 DFIG data

Parameter	Value
Stator resistance	0.0034 Ω
Rotor resistance	0.003 Ω
Stator leakage reactance	0.055 Ω
Rotor leakage reactance	0.042 Ω
Magnetizing reactance	1.6 Ω

8. REFERENCES

1. L.H.Hansen, L. Helle, F. Blaabjerg, E. Ritchie, S. Munk-Nielsen, H. Bindner, P. Sørensen, and B. Bak-Jensen, "Conceptual Survey of Generators and Power Electronics for Wind Turbines," Risø Nat. Lab., Roskilde, Denmark, Tech. Rep. Risø-R-1205(EN), Dec. 2001.
2. Andres E. Feijoo and Jose cidars, 'Modelling of Wind Farms in the Load Flow Analysis'. IEEE Transactions on Power systems, Vol 15, No. 1, February 2000, pp. 110-115
3. Divya K.C. and Nagendra Rao P.S., 'Models for Wind Turbine Generating Systems and their application in Load flow studies'. Electric Power Systems Research, Vol. 76, 2005, pp. 844-856.
4. R.Pena, J.C.Clare and G.M.Asher. 'Doubly fed induction generator using back-to-back PWM converters and its application to variable speed wind energy conversion systems'. IEE proceedings on Electr. Power Appl. Vol.143, N0.3, 1996, pp.231-241.
5. L.Holds worth, X.G.Wu, J.B.Ekanayake and N.Jenkins:"Direct solution method for initialising doubly-fed induction wind turbines in power system dynamic models". IEE Proceedings Generation, Transmission and Distribution. Vol.150, No.3, May-2003. Pp.334-341.
6. L.Holds worth, X.G.Wu, J.B.Ekanayake and N.Jenkins. 'Comparison of fixed speed and doubly fed wind turbines during power system disturbances'. IEE Proceedings Generation, Transmission and Distribution, Vol.150, No.3, May-2003, pp.342-352.
7. Sloomweg.J.G, Polider.H and Kling.W.L (2001), 'Initialization of wind turbine models in power system dynamic simulations', IEEE Porto power tech conference, 10th – 13th September, Portugal.
8. Z. Lubosny, Wind Turbine Operation in Electric Power Systems Advanced modeling, Springer Verlag, 2003.
9. S.N.Bhadra, D.Kastha and S.Banerjee:" Wind Electrical Systems". Oxford University Press, 2007.